INVESTIGATION OF RADARSAT-2 AND TERRASAR-X DATA FOR RIVER ICE CLASSIFICATION

Stephane Mermoz[1,2], *Sophie Allain*[1], *Monique Bernier*[2] *and Eric Pottier*[1]

[1] IETR Laboratory, UMR CNRS 6164, University of Rennes 1
Campus de Beaulieu Bâtiment 11D, 263 Avenue Général Leclerc, 35042 Rennes Cedex, France
[2] INRS ETE, University of Québec
490 rue de la Couronne, Québec (Québec), G1K9A9, Canada

ABSTRACT

To date, monitoring of river ice using remote sensing has mainly focused on the use of mono-polarized and multi-polarized C-band radar data only. In this paper, Support Vector Machine (SVM) classifications using polarimetric parameters are tested to identify types of river ice. Classification algorithms are validated on the newly available C-band Radarsat-2 and X-band Terrasar-X data to investigate the potential of this new imagery, acquired in winter 2009. An electromagnetic model is improved to simulate the polarimetric response of a river ice cover to understand the interactions of the radar signal with the ice cover. At C-band, using dual-polarized data over mono-polarized data increases by 23.9% the final classification producer accuracy. Furthermore, the best producer accuracy is 91.6% when using dual-pol data at C-band, which stand for a gain of 2.2% compared to dual-pol data at X-band

Index Terms— River ice, Classification, PolSAR data, Electromagnetic model

1. INTRODUCTION

The development of ice covers on large rivers can result in ice jamming and flooding of large areas. The severity and economic impact of floods related to ice jams is exacerbated by the danger of post-flooding freeze-up. Satellite based monitoring services offer an ideal solution allowing decision makers to collect information on river ice repeatedly and consistently throughout the ice season. To date, monitoring of river ice through remote sensing has mainly focused on the use of mono-polarized and multi-polarized C-band radar data [1][2]. New satellites such as Radarsat-2 host a number of new capabilities, such as super fine resolution, dual polarization mode and full polarimetric data, which will enhance river ice monitoring services. Of particular interest are the identification of scattering properties of different ice types and the improvement of ice type classification accuracy. It is expected that the results from this investigation will directly improve the quality and efficiency of satellite-based river ice monitoring. This work evaluates the potential of dual-polarized SAR data at X- and C-band for improved river ice classification. The first part of this paper focuses on the polarimetric theory. Then, interactions between river ice and signal are described, followed by a description of field and SAR data. The fifth part focuses on the classification used (SVM). Finally, the results are presented and compared with ground-truth data.

2. POLARIMETRIC THEORY

The polarimetric radar measures the response of a medium in the form of a scattering matrix S, expressed in the linear (H,V) basis, as:

$$S = \begin{bmatrix} S_{HH} & S_{HV} \\ S_{VH} & S_{VV} \end{bmatrix} \qquad (1)$$

The four elements S_{HH}, S_{HV}, S_{VH} and S_{VV} are complex numbers. In the monostatic case, $S_{HV} = S_{VH}$. Thus, polarimetric data set can be represented as a target vector k. The covariance matrix C has a complex Wishart distribution. k and C can be defined as:

$$S = \begin{bmatrix} S_{HH} & \sqrt{2}S_{HV} & S_{VV} \end{bmatrix}^T \text{ and } C = kk^{*T} \qquad (2)$$

where the superscript "T" denotes the matrix transpose. The span is a quantity giving the total power received by the four channels of a polarimetric radar system:

$$span = |S_{HH}|^2 + |S_{HV}|^2 + |S_{VH}|^2 + |S_{VV}|^2 \qquad (3)$$

In dual-polarized configuration (HH-VV),

$$span = |S_{HH}|^2 + |S_{VV}|^2 \qquad (4)$$

The correlation between HH and VV, sensitive to the scattering mechanisms, is expressed as:

$$\rho_{HHVV} = \frac{|S_{HH}S_{VV}^*|}{\sqrt{|S_{HH}|^2}\sqrt{|S_{VV}|^2}} \qquad (5)$$

The entropy H is a measure of target disorder [3], with $H = 1$ for a completely random target for which all eigenvalues

are equal, and $H = 0$ for a simple target (single scatterer). Finally, H and θ parameters are given by:

$$H = -\sum_{i=1}^{3} \frac{\lambda_i}{\lambda_1 + \lambda_2 + \lambda_3} \log_2 \frac{\lambda_i}{\lambda_1 + \lambda_2 + \lambda_3} \quad (6)$$

$$\theta = -\sum_{i=1}^{2} \frac{\lambda_i}{\lambda_1 + \lambda_2} \log_2 \frac{\lambda_i}{\lambda_1 + \lambda_2} \quad (7)$$

This last parameter can be used only for dual-polarized data.

3. INTERACTION BETWEEN RIVER ICE AND SIGNAL

The backscattered signal from the ice cover is composed of surface and volume scattering contributions. The surface scattering is mainly influenced by the snow-ice and ice-water interface roughness and dielectric constant [4]. Volume scattering is caused by all the impurities inside the ice matrix. Air inclusions are usually the most significant scatterers [5]. The snow ice is a superimposed ice which contains closely bunched spherical air bubbles (0.001-0.25cm). The thermal ice contains irregularly spaced spherical or tubular air bubbles (0.1-0.3cm). The frazil ice contains closely bunched spherical and irregular bounded air inclusions (0.2-1.3cm). For this study, four classes are defined: the Open Water (OW), the Intact Ice (II) which contain thermal ice or fused layers of thermal and frazil ice, the floating Frazil Ice (FI) which include slush, pans and floes, and the Consolidated Ice (CI) which is a mix of different ice types and has typically very rough air-ice interface.

Gherboudj [6] has developed a backscatter model describing the river ice medium in order to understand the interactions of the radar signal with the river ice cover. The proposed model is based on the Vector Radiative Transfer (VRT) theory and the Integral Equation Model (IEM) [7]. The model, built to estimate the total response (HH, VV and HV channels) from the ice cover, is improved to be a full polarimetric model (hence including the phase values). This model requires the following input data: ice cover thickness, ice cover porosity p, size of scatterers (radius r and length h) within each ice layer and boundary characteristics of the main medium (surface height standard deviation ($k\sigma$), correlation length (kL_c) and correlation function) (k is the wave number of the host medium). The contribution of each the above mentioned parameters to the overall backscattering response was assessed using a series of modelling experiments, and the main results are presented in section 6.1 and in Fig.1.

4. FIELD AND SAR DATA

4.1. Field data

The test site is the Saint-Francois River (45^o50N ; 72^o22W), located in southern Quebec and upstream from the town of
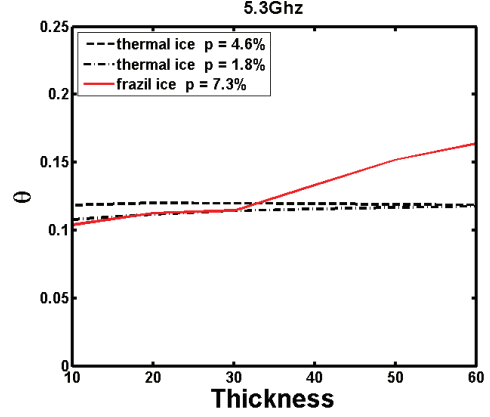

Fig. 1. Simulation results for three ice covers. ($k\sigma$,kL_c) for both air-ice and ice-water boundaries is (0.15,1)
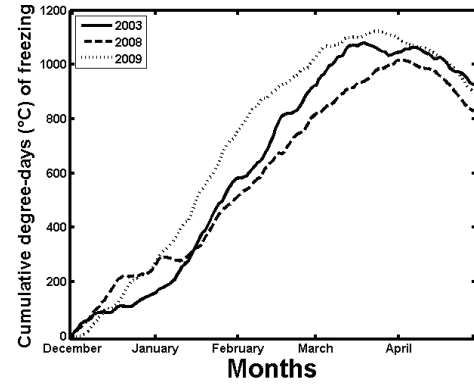

Fig. 2. Weather conditions for winter 2003, 2008 and 2009

Drummondville. The stream flow is roughly south to north. The study section is approximately 30km long. Channel width varies from 100m to 850m and the depth reaches 2-4m in general. Ground-truth data have been measured the same days as the satellite overpass on the Saint-Francois River in Winters 2008 and 2009. Ice cores were extracted and analyzed for ice type and porosity. Ice cores and ground photos are conjointly used to establish validation sites for the ice cover classification. Ice thicknesses (between 0.3m-2m) were also measured using a Ground Penetrating Radar. The cumulative freezing-degree days (Fig.2) also provide a useful tool that can explain the presence of frazil and air inclusions in the ice cover. This parameter has higher values for the 2009 season. Such values indicate the high rate of freezing required for frazil formation to occur, and show an increase in the amount and/or the size of air bubbles.

4.2. SAR data

Single-polarized Radarsat-1 images were acquired on February 3 and 27 and on March 6 2009. Furthermore, five Radarsat-2 full polarimetric images in quad-fine mode were also acquired. Three datasets were acquired over the Saint-

Francois River on February 5 and 28 2009 and on March 14 2009. Due to its system configurations, the German satellite Terrasar-X also provides an excellent data base regarding the monitoring of river ice distribution as well as for its characterization. In fact, because of the low dielectric constant of the river ice, even high frequencies will penetrate it. Short wavelengths (9.65GHz) and polarimetric data contribute to the separation of volume and surface scattering. A total of four coherent dual-polarized Terrasar-X images were acquired over the Saint-Francois River on February 17 2008, March 10 2008, February 3 2009 and February 25 2009. Each time, Single-Look Complex (SLC) are available. Data have been multi-looked. A 7*7 window size Lee filter was also applied to reduce the speckle effect.

5. CLASSIFICATION USED

Support Vector Machines (SVM) is a useful technique for data classification and recently became one of the most popular classification methods. It has been used in a wide variety of applications such as text classification, facial expression recognition, gene analysis and many others. The theoretical foundation of this method is given by statistical learning theory. SVM can be thought of as a method for constructing a special kind of rule, called a linear classifier, in a way that produces classifiers with theoretical guarantees of good predictive performance (the quality of classification on unseen data). SVM delineates two classes by fitting an optimal separating hyperplane to the multidimensional feature space. This optimization bases on structural risk minimization and tries to maximize the margin between the hyperplane and the closest training data points, the so-called support vectors. Thus, SVM only considers training samples close to the class boundary and might work well with small sample sets. For linearly not separable classes the input data are mapped into a high dimensional space wherein the newly spread data point distribution enables the fitting of a linear hyperplane. A detailed description on the concept of SVM is given in [8].

6. RESULTS

6.1. Simulations of the electromagnetic model

Superposing snow ice (thickness = 30cm, r = 0.05cm and p = 18.2%) and thermal ice (r = 0.05cm) causes a small increase in θ (1.1% with p = 1.8% at C-band with thickness ranging from 30cm to 40cm) when the porosity and the thickness increase (Fig.1). An increase in the frequency leads to a small increase in θ. Superposing snow ice and frazil ice (r = 0.2cm) causes a strong increase in θ (16.6% with p = 7.3% at C-band with thickness ranging from 30cm to 40cm) when the porosity and the thickness increase (Fig.1). θ is logically higher at X-band than at C-band. Even at higher frequencies, the snow ice causes a very small increase in θ when the porosity and the

thickness increase. Thus, the snow ice is almost transparent for radar signals, and the increased θ observed for snow ice superposed on thermal ice is caused by the multiple scattering occurring between scatterers of different ice layer. These results confirm the observations of the polarimetric parameters behaviour depending on the type of ice.
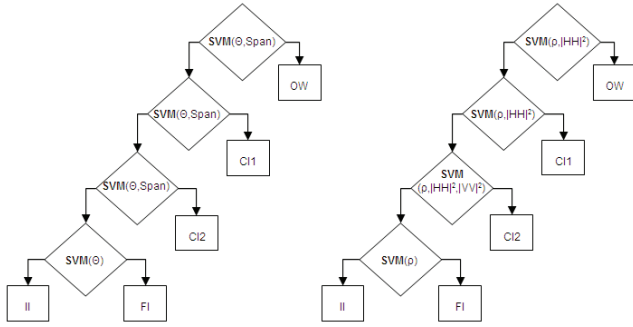
6.2. Classifications

Classes are derived using the total power (span) and θ parameter at X-band, and intensity values in HH and VV and ρ parameter at C-band (Fig.3). For each ice class, training sites are selected and their probability density functions were plotted for different polarimetric parameters. The above parameters are chosen because the corresponding Bhattacharrya and Chi2 distances separating the density probability functions of the training sites are the shortest. Furthermore, the θ and ρ parameters are independent of the span information. These parameters are thus complementary.

The results in Fig.4a demonstrate that dual-polarized (HH-VV) C-band data produce superior classification results over the dual-polarized (HH-VV) X-band data. Using dual-polarized dataset at C-band versus X-band causes an increase in the producer accuracy (from 2.2% to 3.8% depending on the dataset) and in the user accuracy (from 10.8% to 14.4%). The results in Fig.4b demonstrate that at C-band, dual-polarized (HH-VV) SAR data produce superior classification results over the single-polarized data, causing a strong increase in the producer accuracy (from 15.9% to 23.9%) and in the user accuracy (from 17.1% to 22.5%). A confusion matrix, which illustrates the results of the SVM algorithm on the 5 February 2009 Radarsat-2 dataset, is shown as an example in Fig.5. There are few open water pixels but they are well classified. Consolidated ice could be better classified (81.4% of producer accuracy). The algorithm is stable in the detection of the intact ice (95.9% of producer accuracy) but overestimates it (66.7% of user accuracy). Fig.6 shows the result of a five-class hierarchical classification. A fifth class was added to detect the eventual presence of frazil floes on the river. However, on February 5, 2009, no frazil floes were seen during the field campaign (February 4-5) and open water could (in blue) only be noticed on the northern section of the river. The two main ice classes shown on this classification are Intact Ice (thermal ice only) and Consolidated Ice. The ice core samples also confirm the presence of those two types of ice. The zoomed area shows that in case of Radarsat-2 dataset, the detected open water area is more homogenous than Radarsat-1 dataset.

7. CONCLUSION

The major objectives of this project were to evaluate the utility of dual-polarized SAR to develop river ice classification algorithms data for river ice monitoring. Various classification algorithms have been compared and the SVM is retained because it shows a greater ability to generalise. The

Fig. 3. SVM classification scheme at (a) X-band (b) C-band. In this study, CI1 and CI2 are merged. OW=Open Water; CI=Consolidated Ice; II=Intact Ice; FI=Frazil Ice


(a)   (b)
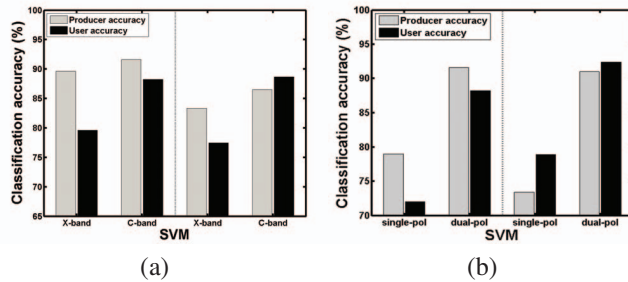
Fig. 4. (a) Validation with dual-pol February 3-5 (left) and 25-28 (right) 2009 SAR data. (b) Validation with C-band February 3-5 (left) and 27-28 (right) 2009 SAR data

	OW	CI	II	Total Possible	Producer accuracy %	Mapping accuracy %
OW	158	0	4	162	97.5	97.5
CI	0	1245	285	1530	81.4	80.1
II	0	25	579	604	95.9	64.8
Total Possible	158	1270	864			
User accuracy %	100	98	66.7			

Fig. 5. SVM confusion matrix with dual-pol February 5 2009 SAR data at C-band

availability of Radarsat-2 data in 2009 provides the opportunity to validate these algorithms and to estimate the potential of polarimetric data for classifying river ice. All classifications of Radarsat-2 SAR data show no ambiguities between water and ice discrimination, contrary to classification with single-polarized data. This work has demonstrated that dual-polarized (HH-VV) SAR data produce superior classification results over the single-polarized data (respectively 15.9% and 23.9% of increase of the producer accuracy). Besides Furthermore, the best producer accuracy is 91.6% when using dual-pol data at C-band, a gain of 2.2% compare to dual-pol data at X-band. In the near future, Radarsat-2 data should provide
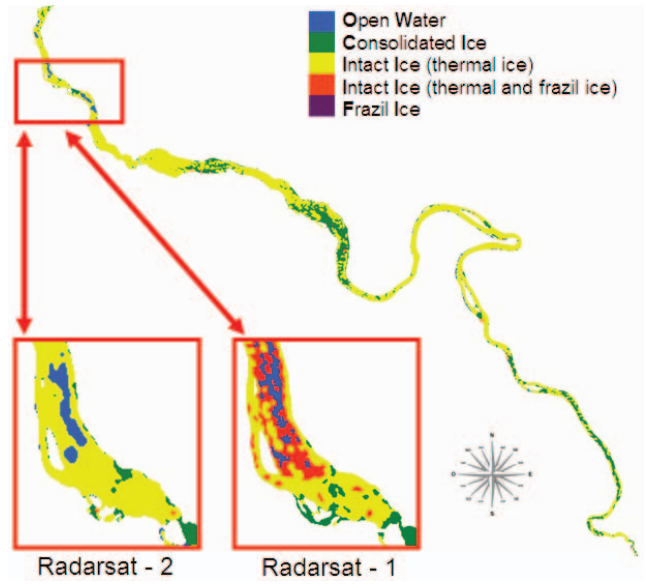
Fig. 6. SVM classification with dual-pol February 5 2009 SAR data at C-band

improved ice edge detection, ice topography and structure information.

8. REFERENCES

[1] Y. Gauthier, F. Weber, S. Savary, M. Jasek, L.M. Paquet, and M. Bernier, "A combined classification scheme to characterize river ice from sar data," in *EARSeL*, 2006, vol. 5, pp. 77–88.

[2] A. El Battay, *Développement d'une approche de Classification Orientée Objet pour une meilleure caractérisation de la glace d'une rivière de taille moyenne à l'aide des images du satellite RADARSAT-1 et d'un Système d'Information Géographique: cas de la rivière Saint-Franois, Québec*, Ph.D. thesis, Institut National de la Recherche Scientifique, Québec, 2006.

[3] S.R. Cloude and E. Pottier, "An entropy based classification scheme for land applications of polarimetric sar," *IEEE*, vol. 35, pp. 68–78, 1997.

[4] M.L. Bryan and R.W. Larson, "The study of fresh water lake ice using multiplexed imaging radar," *Journal of Glaciology*, vol. 14, pp. 445–457, 1975.

[5] B. Michel and M. Drouin, "Formation, classification et proprits mcaniques de la glace," in *Sixième colloque d'initiation aux principes de l'hydrologie. GCE-72-08-01*, 1972, p. 18.

[6] I. Gherboudj, M. Bernier, and R. Leconte, "Validation of a backscatter model of a river ice covers using radarsat-1 images," in *IEEE*, 2007, pp. 1087–1090.

[7] A.K. Fung, "Microwave scattering and emission models and their applications," Artech House, Inc., Bston, London, 1994, p. 573.

[8] V. Vapnik, "The nature of statistical learning theory," Springer-Verlag, New-York, 1995.